

# Tunable Gas Sensing Gels by Cooperative Assembly

Abid Hussain, Ana T. S. Semeano, Susana I. C. J. Palma, Ana S. Pina, José Almeida, Bárbara F. Medrado, Ana C. C. S. Pádua, Ana L. Carvalho, Madalena Dionísio, Rosamaria W. C. Li, Hugo Gamboa, Rein V. Ulijn, Jonas Gruber,\* and Ana C. A. Roque\*

The cooperative assembly of biopolymers and small molecules can yield functional materials with precisely tunable properties. Here, the fabrication, characterization, and use of multicomponent hybrid gels as selective gas sensors are reported. The gels are composed of liquid crystal droplets self-assembled in the presence of ionic liquids, which further coassemble with biopolymers to form stable matrices. Each individual component can be varied and acts cooperatively to tune gels' structure and function. The unique molecular environment in hybrid gels is explored for supramolecular recognition of volatile compounds. Gels with distinct compositions are used as optical and electrical gas sensors, yielding a combinatorial response conceptually mimicking olfactory biological systems, and tested to distinguish volatile organic compounds and to quantify ethanol in automotive fuel. The gel response is rapid, reversible, and reproducible. These robust, versatile, modular, pliant electro-optical soft materials possess new possibilities in sensing triggered by chemical and physical stimuli.

## 1. Introduction

Supramolecular self-assembly is attracting significant interest as an approach to functional materials design, with tremendous, mostly untapped opportunities in creating new types of sensors. There is clear evidence that cooperative assembly of polymers and small molecules endows composites with new properties, not found in the individual components.<sup>[1]</sup> So far, this coassembly approach has largely focused on tuning mechanical properties, but not in engineering supramolecular recognition.<sup>[2]</sup> Molecular recognition and detection of analytes in the gas phase is becoming increasingly relevant in such diverse areas as medicine,<sup>[3]</sup> manufacturing industry,<sup>[5]</sup> security,<sup>[6]</sup> environment,

Dr. A. Hussain, A. T. S. Semeano, Dr. S. I. C. J. Palma, Dr. A. S. Pina, J. Almeida, B. F. Medrado, A. C. C. S. Pádua, Dr. A. L. Carvalho, Prof. A. C. A. Roque  
UCIBIO

REQUIMTE  
Departamento de Química  
Faculdade de Ciências e Tecnologia  
Universidade Nova de Lisboa  
2829-516 Caparica, Portugal  
E-mail: cecilia.roque@fct.unl.pt

A. T. S. Semeano, B. F. Medrado, Dr. R. W. C. Li, Prof. J. Gruber  
Departamento de Química Fundamental  
Instituto de Química da Universidade de São Paulo  
Av. Prof. Lineu Prestes  
748 CEP 05508-000, São Paulo, SP, Brasil  
E-mail: jogruber@iq.usp.br

Dr. A. S. Pina, Prof. R. V. Ulijn  
Advanced Science Research Center (ASRC)  
City University of New York  
New York 10031, USA

Prof. M. Dionísio  
LAQV  
REQUIMTE  
Departamento de Química  
Faculdade de Ciências e Tecnologia  
Universidade Nova de Lisboa  
2829-516 Caparica, Portugal

Dr. R. W. C. Li  
Centro Universitário Estácio Radial de São Paulo  
Vila dos Remédios  
CEP 05107-001 São Paulo, SP, Brasil  
Prof. H. Gamboa  
Laboratório de Instrumentação  
Engenharia Biomédica e Física da Radiação (LIBPhys-UNL)  
Departamento de Física  
Faculdade de Ciências e Tecnologia da Universidade Nova de Lisboa  
Monte da Caparica  
2892-516 Caparica, Portugal

Prof. R. V. Ulijn  
Hunter College  
Department of Chemistry and Biochemistry  
695 Park Avenue, New York, NY 10065, USA  
Prof. R. V. Ulijn  
PhD Programs in Chemistry and Biochemistry  
The Graduate Center of the City University of New York  
New York, NY 10016, USA

 The ORCID identification number(s) for the author(s) of this article can be found under <https://doi.org/10.1002/adfm.201700803>.

DOI: 10.1002/adfm.201700803

agricultural, and food sciences,<sup>[7]</sup> as well as for the fundamental understanding of biological processes.<sup>[8]</sup> Electronic noses (e-noses), specially those based on metal oxide semiconductors, are currently the most widespread devices for detection of gases and volatile organic compounds (VOCs).<sup>[9,10]</sup> E-noses comprise of an array of chemical sensors with partial selectivity coupled to an appropriate pattern recognition system, capable of recognizing simple or complex odors and greatly resembling the biological olfactory system.<sup>[11]</sup> The lack of selectivity of chemical sensors has been one of the key challenges, minimized with the introduction of selective elements as biological receptors,<sup>[12,13]</sup> engineered peptides,<sup>[14]</sup> or biomimetic nanostructures.<sup>[15]</sup>

Ionic liquids (ILs)<sup>[16,17]</sup> and liquid crystals (LCs)<sup>[18]</sup> are molecules with self-assembly potential, which have been individually assessed for gas sensing.<sup>[19,20]</sup> Ionic liquids present substantial structural and functional diversity, being appealing for the generation of selective gas sensing materials.<sup>[21]</sup> Liquid crystals are able to report and amplify interfacial events at the nanoscale and widely explored for the detection of analytes in aqueous solutions.<sup>[22,23]</sup> The potential of LCs for the detection of gases and VOCs has been acknowledged recently. In the examples reported thus far, LCs are typically used as planar films deposited onto chemically treated glass surfaces. The surface-aligned LCs are then perturbed due to the interaction of VOCs with chemical groups on the anchoring surfaces,<sup>[24,25]</sup> on the LC films,<sup>[26]</sup> or with chemical dopants,<sup>[27]</sup> giving rise to changes in the optical pattern of the LCs visible under polarizing optical microscopy (POM). The encapsulation of LCs into droplets increases the available surface area, avoids extensive surface treatments to define the initial LC orientation, and takes advantage of self-assembled and phase-segregated LC structures.<sup>[28,29]</sup> This approach has been particularly prominent for LC sensing in aqueous solutions,<sup>[30–33]</sup> but the optical observation of free-floating droplets remains a challenge.<sup>[34]</sup> Despite the important advances brought up by recent works,<sup>[35,36]</sup> the full potential of LC droplets as gas sensing elements remains largely unfulfilled mainly due to challenges in stabilizing the LC composites and introducing selectivity toward distinct VOCs.

Here, we report the discovery of tunable multicomponent hybrid gels encapsulating liquid crystal-ionic liquid droplets (LC-IL droplets), and explore their potential as stable combinatorial materials for gas sensing. The uniqueness of this approach is that each component of the gel plays a distinct but yet cooperative role in structure and function, with unprecedented diversity and potential to tune the materials for flexible optoelectronic devices.

## 2. Results and Discussion

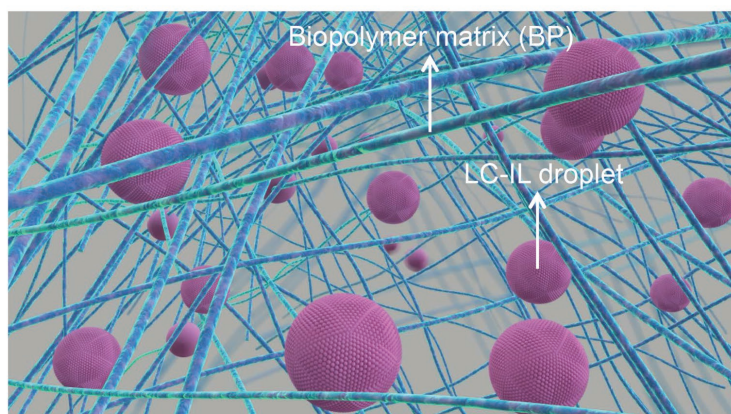
The cooperative hybrid gel concept was initially tested with composites made of gelatin, 1-butyl-3-methylimidazolium dicyanamide ([BMIM][DCA]) and 4-cyano-4'-pentylbiphenyl (5CB) in the presence of water. The LC-IL droplets self-assembled in the presence of water, with the LCs displaying preferentially a radial configuration (Figure 1 and Figure S1, Supporting Information). The ionic liquid promotes the anchoring and alignment of the LC, either through the establishment of hydrophobic interactions between the hydrophobic component of LC

and the apolar tail of the ionic liquid, or through the establishment of electrostatic interactions between the cyano moiety of LC and the charged components of the ionic liquid.<sup>[37]</sup> The net result is the encapsulation of the LC in LC-IL droplets, resembling self-assembling processes of amphiphiles and other surfactants in the presence of LCs.<sup>[38–40]</sup> In addition, the ionic liquid promotes gelatin dissolution while establishing non-covalent interactions with the biopolymer chains, most probably ionic interactions and hydrogen bonds.<sup>[41,42]</sup> It has been proposed that the core of gelatine ionogels is filled with ionic liquid bilayers and micelles. In hybrid gels, it is likely that most ionic liquid micelles are not empty and carry the LC optical probe<sup>[42]</sup> (Figure 1). Despite knowing that in gelatine ionogels the presence of the ionic liquid and the voids formed tend to weaken the network structure, we observed that hybrid gels were robust.

Hybrid gels are transparent, self-supporting, and flexible matrices with mechanical stability, within which the LC-IL droplets are confined. Gels remained stable when stored at ambient conditions for at least 3 months (Figures S1 and S2, Supporting Information), with no significant cracking or shrinking over time as observed in hydrogels, probably due to the low vapor pressure of ionic liquids. As the hybrid gels provide a combinatorial platform to generate customizable composites, each individual component—biopolymer, ionic liquid, and LC—were varied.<sup>[43]</sup> For all hybrid gels prepared (over 12 distinct compositions), robust films were obtained and encapsulated LC-IL droplets were observed, containing LC molecules with a preferential radial arrangement (Figures S5 and S6, Supporting Information).

The optical and morphological properties of hybrid gels were further assessed (Figure 1 and Figure S3, Supporting Information). The control materials studied included C0 (containing gelatin and water), C1 (containing gelatin, ionic liquid, and water), and C2 (containing gelatin, liquid crystal, and water). Both control films C0 and C1 possess smooth surfaces with granule-like irregularities. The C2 control film presents a rough surface, with symmetrical droplets and holes, and visible LC droplets in a bipolar configuration. Hybrid gel films are smoother, with symmetrical and smooth protuberances corresponding to the LC-IL droplets. Mechanical properties were assessed by frequency-dependent rheometry measurements confirming the gel-like nature of the hybrid gel, with a constant storage modulus ( $G'$ ) of  $\approx 10^3$  Pa, similar to C1 (Figure 2A–D and Figure S4, Supporting Information). Temperature increase has minimal influence on the rheological properties of the hybrid gel and C1, but it causes structure reorganization in control C2. Significant structural differences are noted between water-based gelatin films (without and with LC, C0 and C2), and ionic liquid-containing gelatin films (C1 and hybrid gels), as observed by X-ray diffraction (XRD) analysis (Figure 2E–H). The water-based gelatin films (C0) exhibited two distinct scattering rings, at  $\approx 10.7$  and  $4.8$  Å resolution, and an additional faint, but still detectable, scattering at  $2.8$  Å, as previously reported.<sup>[41]</sup> In gelatin hydrogels each chain is twisted in a left-handed helix conformation and three such helices supercoil together to form the right-handed triple helix.<sup>[44]</sup> The high-resolution ring arises from the residue periodicity of each helix turn ( $2.9$  Å), whereas the low resolution ring ( $10.7$  Å) corresponds to

**a Hybrid Gel**



**LC-IL droplet**

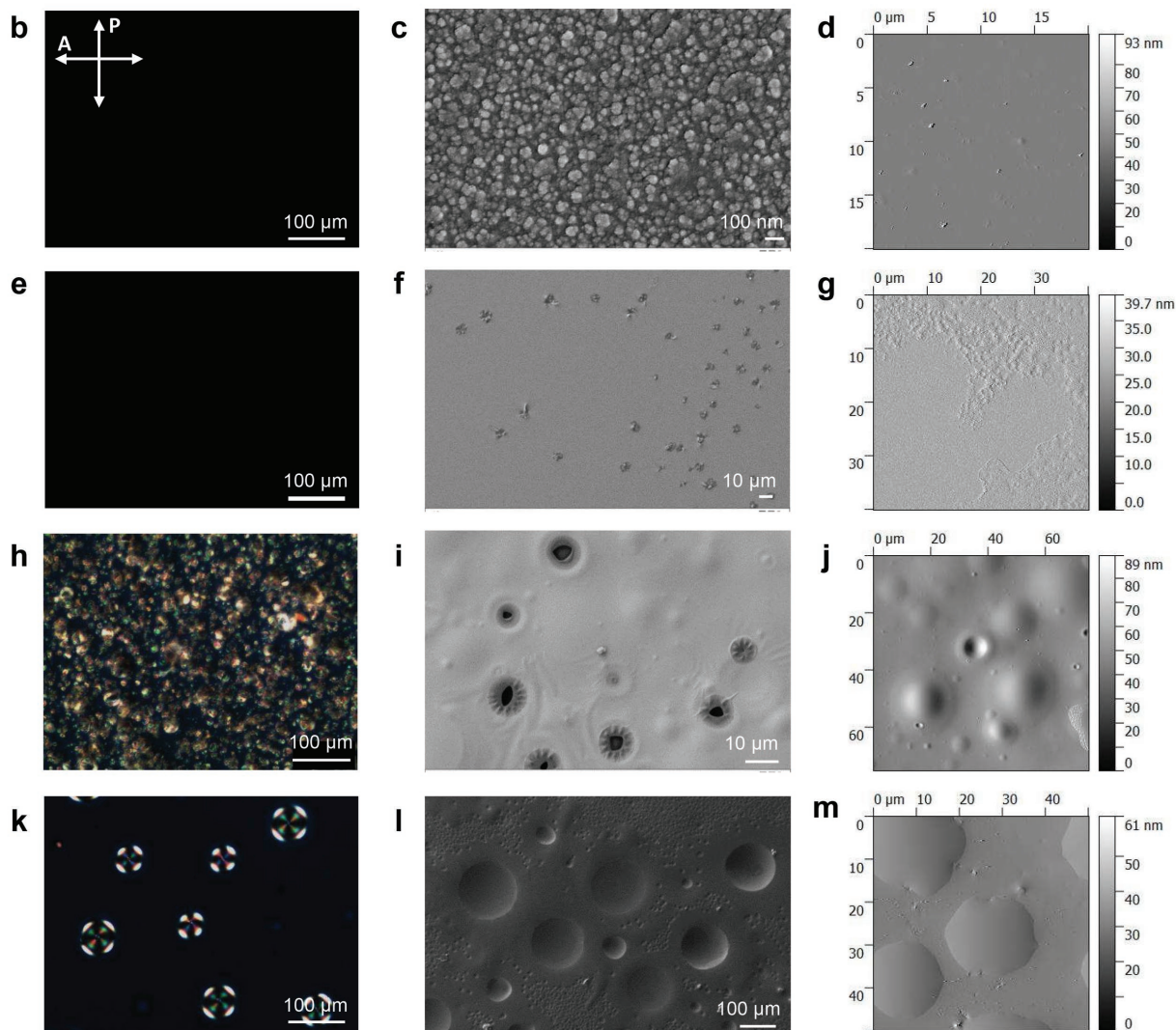
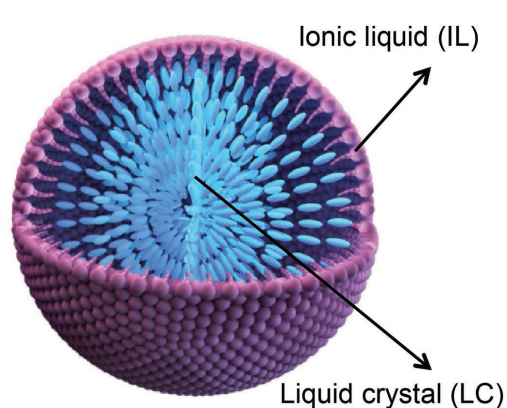


**Figure 1.** Optical and morphological characterization of hybrid gel films composed of gelatin, [BMIM][DCA], 4-cyano-4'-pentylbiphenyl (5CB), and water. a) Schematic illustration of the organization of hybrid gels, showing the liquid crystal and ionic liquid in droplets (LC-IL droplets) supported in the biopolymer-ionic liquid network. b,e,h,k) Polarizing optical microscopy (POM) images with crossed polarizers. c,f,i,l) Scanning electron microscopy (SEM) images of Au/Pd coated films. d,g,j,m) Atomic force microscopy (AFM) images. b–d) C0 film: gelatin and water. e–g) C1 film: gelatin, [BMIM][DCA], and water. h–j) C2 film: gelatin, 5CB, and water. k–m) Hybrid gel film: gelatin, [BMIM][DCA], 5CB, and water.



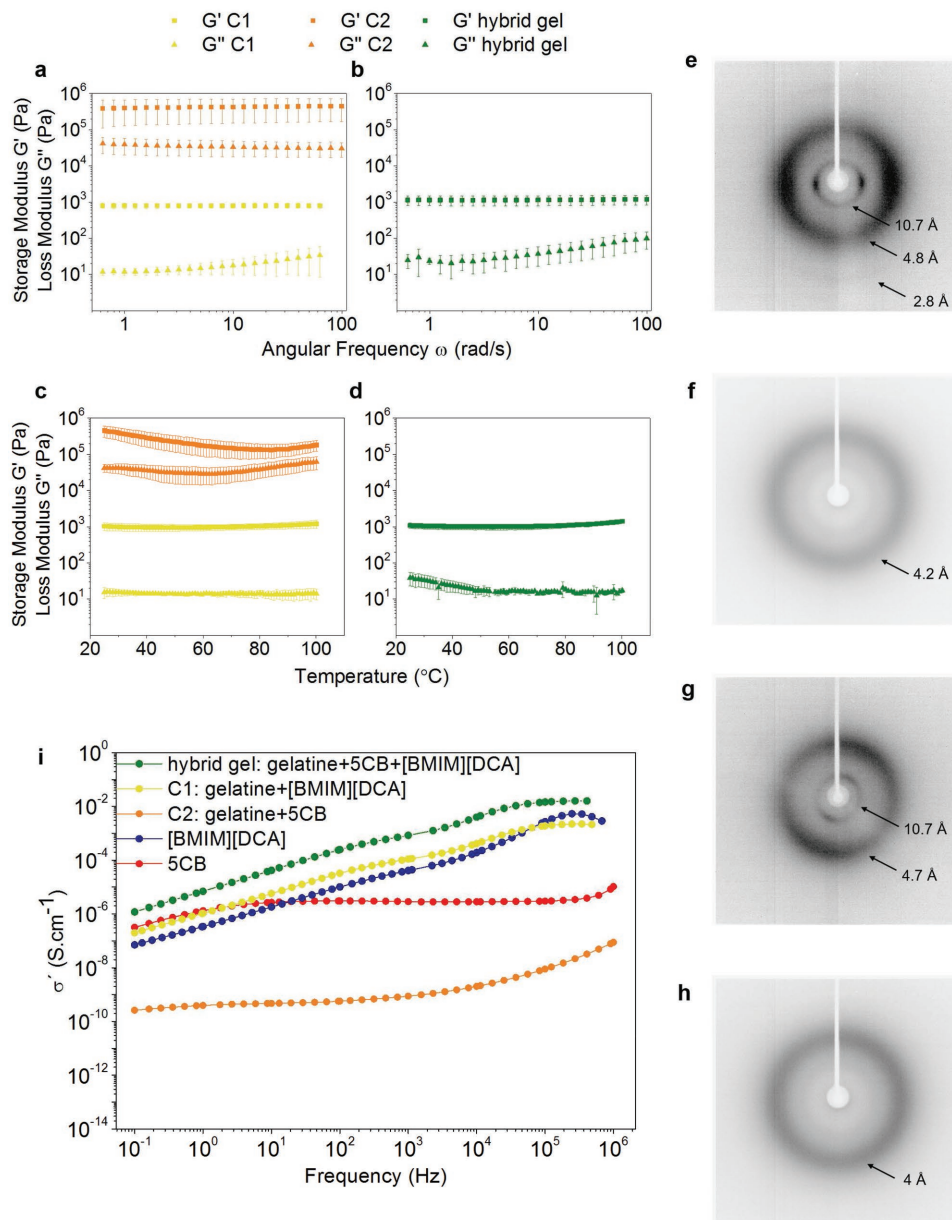


**Figure 2.** Mechanical, structural, and electrical conductivity properties of hybrid gel films composed of gelatin, [BMIM][DCA], 4-cyano-4'-pentylbiphenyl (5CB), and water. a–c) Analysis of viscoelastic properties ( $N = 3$ ). Surface shear storage ( $G'$ ) and loss ( $G''$ ) moduli as a function of angular frequency for: a) control (C1 and C2) thin films in the linear region (strain 2.59% for C1 and 0.12% for C2); b) hybrid gel film (strain 0.27%). Variation of surface shear storage ( $G'$ ) and loss ( $G''$ ) modulus with the temperature for: c) control (C1 and C2) and d) hybrid gel films ( $1 \text{ rad s}^{-1}$ ). e–h) X-ray scattering images of control (e, C0; f, C1; g, C2) and hybrid gel (h) films. i) Real part of the conductivity spectra for the materials and neat constituents (298 K; data normalized for the water content (% w/w)).

the diameter of the superhelix aggregate of the hydrogel.<sup>[41,42]</sup> Upon incorporation of the LC (C2 film) the high-resolution ring becomes less visible but not the  $10.7 \text{ \AA}$ , which indicates that gelatin's aggregation state is unaffected. When ionic liquid is added to the composite, a drastic change is observed in the detected X-ray scattering. Gelatin ionogels lack the structural periodicity characteristic of gelatin hydrogels, both at the gelatin left-handed helix and right-handed superhelix levels, due to the interactions between gelatin and ionic liquids.<sup>[41]</sup> This further corroborates the critical role of the ionic liquid in the

reorganization of gelatin chains, namely in weakening the gel matrix network.<sup>[42]</sup>

The possibility to employ the hybrid gels as sensorial elements in gas sensing was further assessed. A hybrid gel film was sequentially exposed to vapors from organic solvents representative of distinct groups (e.g., ketones, alcohols, aliphatic, aromatic and halogenated compounds, 29%–39% (mol/mol) except toluene (6%)) and observed by POM (Figure 3 and Figure S7, Supporting Information). After VOCs exposure, the molecular order of the LCs inside the droplets typically altered

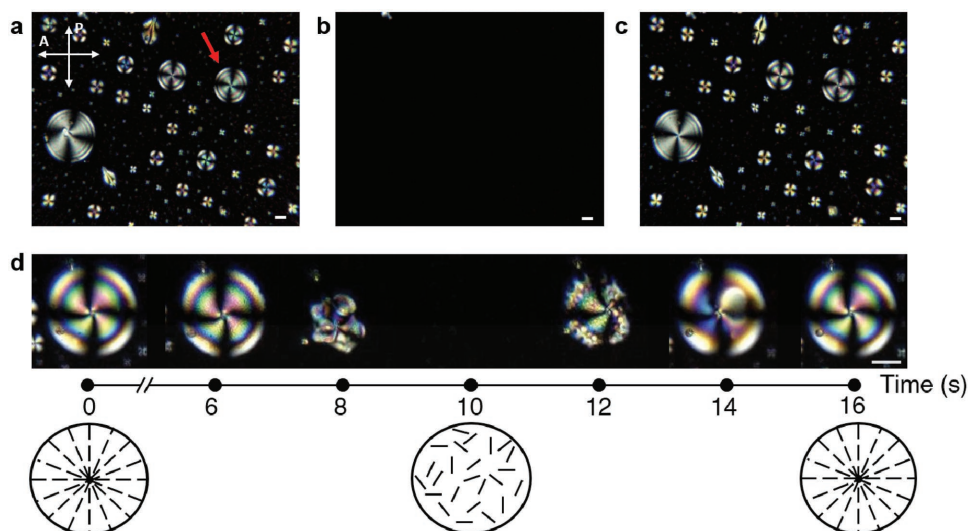


**Figure 3.** Optical response of hybrid gel films when exposed to air saturated in chloroform. Hybrid gel films composed of gelatin, [BMIM][DCA], 4-cyano-4'-pentylbiphenyl (5CB), and water were observed by POM, with crossed polarizers. a–c) Before, during, and after exposure to chloroform VOCs for 2 s. The red arrow indicates the droplet pictured in detail in (d). d) Detailed time analysis of the 15  $\mu\text{m}$  diameter droplet highlighted in (a) (exposure begun at  $t = 0$  s). The scale bars in the microscopy images correspond to 5  $\mu\text{m}$ .

from radial to isotropic. Consequently, the intensity of transmitted light decreased. In the recovery period, the reverse path was noted (Video S1, Supporting Information). This optical response was rapid (of the order of seconds), reversible, and reproducible. The response and recovery profiles were different for each solvent tested, mainly the time and rate required for gel reorganization, and the pattern of LC reorganization as observed by POM (Figure 3 and Figure S7B–I, Supporting Information). For example, the time required for complete isotropy within all LC-IL droplets is similar for hexane, chloroform, and acetone (maximum 20 s), but longer for methanol (40 s). Also, after exposure to vapors from protic solvents (e.g., methanol and ethanol), some LC-IL droplets dynamically rearranged into smaller units or relocated within the gel, suggesting a perturbation of the gelatin chains and ionic liquids configuration in the matrix. Critically, this effect did not impair the subsequent response of the hybrid gel to an aromatic hydrocarbon as toluene (Figure S7C–I, Supporting Information).

Several phenomena may explain the different optical responses observed. Hybrid gels have components with distinct properties, namely gelatin is intrinsically hydrophilic, the ionic liquids are amphiphilic and the LCs are mostly hydrophobic. VOC molecules possessing distinct polarities and functional groups adsorb into the hybrid gel film and interact with different affinities with its individual components, thus resulting in LC disorder (Figure S7J, Supporting Information). In the case of hydrophobic apolar VOCs as hexane and toluene, the predominant effect is probably ruled by the interaction of the VOC molecules with the LC, due to structural resemblance (5CB has a pentyl-hydrocarbon chain and a biphenyl moiety). VOC molecules disrupt the radial orientation of the LC as they directly interact by hydrophobic interactions with alike-LC regions, intercalating the oriented LC molecules. As VOCs desorb from the gel, the LC returns to its original orientation, and the LC-IL droplets are maintained in the same position.

In the case of polar and protic solvents (e.g., alcohols), which act as donors and acceptors of electrons, there is also an increase in the fluidity of the gel. Here, the predominant effect is likely ruled by direct interactions of the VOC molecules with the ionic liquid and the gelatin chains. When VOC molecules interact with the ionic liquid, the self-assembled structures are altered and a greater mobility of ionic liquids is observed. This ultimately results in the dynamic reorganization of the LC-IL droplets as a whole, in addition to the disruption of the LC molecular order. For other VOC molecules with intermediate polarity, hydrophobicity, and structures, we believe there are combined mechanisms of interaction with all the gel components, with different degrees of predominance.

The hybrid gels were used as sensitive layers in optical gas sensors of an in-house built e-nose (Figure 4 and Figure S8, Supporting Information). An array of three optical sensors with hybrid gels of distinct compositions, where the ionic liquid and biopolymeric matrix were varied, was sufficient to classify the VOCs from eleven different organic solvents. Here, the optical response is measured as the total intensity of light from a light-emitting diode that reaches the respective light-dependent resistor (LDR) after passing through the hybrid gel and is not dependent on the study of molecular LC transitions in individual droplets.<sup>[35,39]</sup> A fast response of the optical sensors upon exposure to VOCs is observed within 5 s, about 1/3 of the time reported in other works.<sup>[35]</sup> The relative responses were calculated, and used as input variables for principal component analysis, where 2D scatter plot of the first two principal components shows the discrimination of all tested VOCs. It is also notable that the ability of the hybrid gels to respond to VOCs was maintained, even after storage at ambient conditions for a period of 4 years (Figure S2B,C, Supporting Information). In previous reports using LC for gas sensing, stability was achieved in inert atmosphere for up to 6 months.<sup>[25,35]</sup> Furthermore, the hybrid gels where

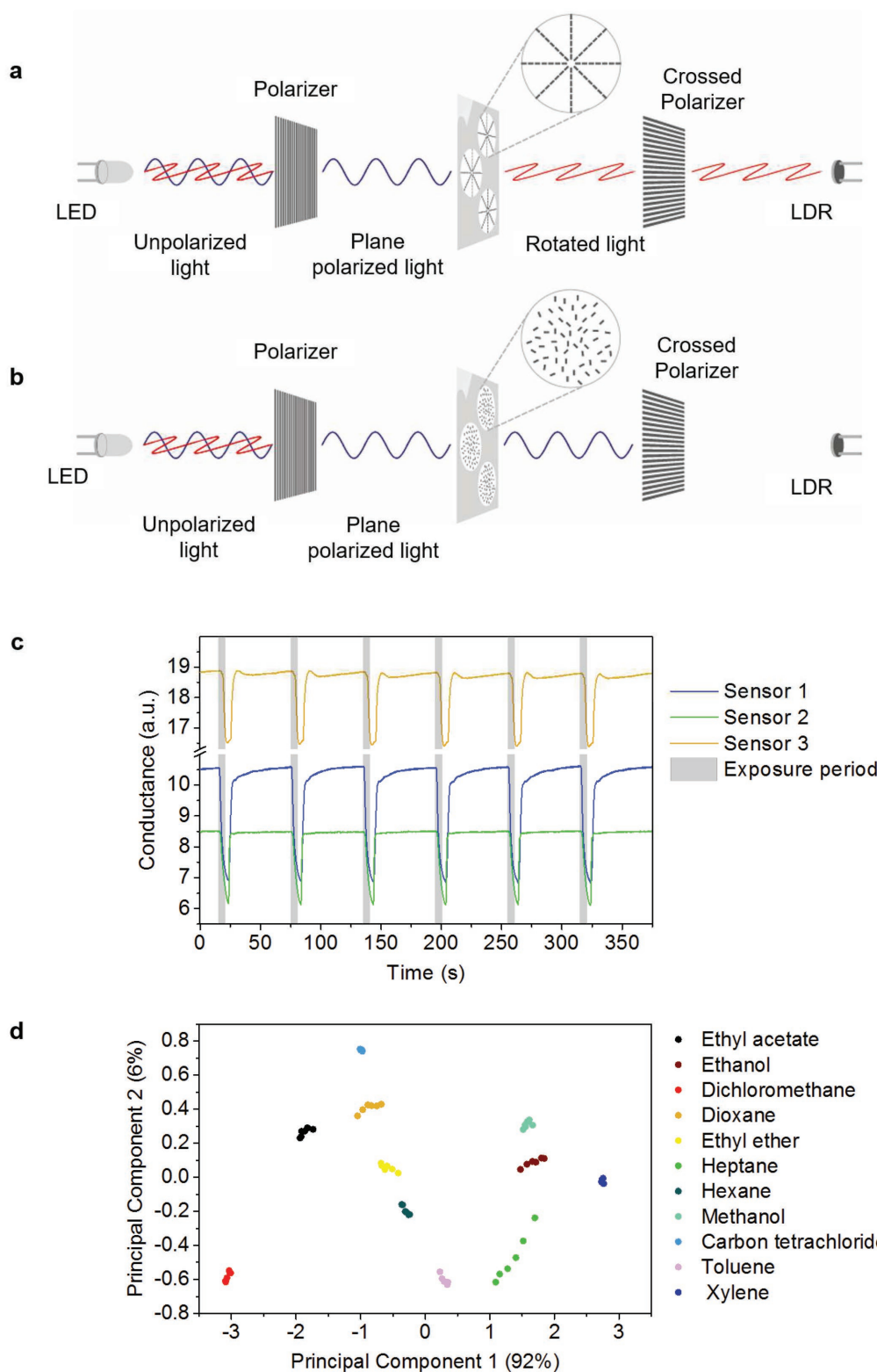


**Figure 4.** Application of the hybrid gels as active layers in optical gas sensors for an electronic nose. a,b) Conceptual representation of the optical component of the electronic nose, with the hybrid gel thin film sandwiched between two crossed polarizers. c) Typical optical response of the electrical nose to VOCs of ethyl acetate, employing three sensors. Exposure periods are highlighted in gray. d) Scatter plot of the two first principal components obtained by principal component analysis of the relative responses of the hybrid gels to 11 different VOCs, allowing to distinguish the solvents in clusters. The contribution of each component is represented between brackets in the respective axes. Hybrid gel compositions: (1) Gelatin, dextran, [BMIM][DCA], 5CB, and water. (2) Gelatin, sorbitol, [BMIM][DCA], 5CB, and water. (3) Gelatin, dextran, [ALOCIM][Cl], 5CB, and water.

also resistant to repeated VOCs exposure (Figure S2D,E, Supporting Information).

The combination of ionic liquid with gelatin yields extremely versatile conductive materials.<sup>[45]</sup> Dielectric relaxation spectroscopy was used to evaluate the conductivity of the hybrid gels. At 298 K, the conductivity of C2 (gelatin and LC) is rather low, increasing by almost six orders of magnitude to  $\approx 10^{-4}$  S cm<sup>-1</sup>, at frequencies close to 1 kHz, when the ionic liquid [BMIM][DCA] is incorporated (C1). For hybrid gels, the conductivity further increases to  $\approx 10^{-3}$  S cm<sup>-1</sup> (Figure 2I and Table S1, Supporting Information). The DC conductivity,  $\sigma_{DC}$ , that corresponds to the translational motion of charge carriers, usually manifests as a plateau in the conductivity plot, but for all materials containing the ionic liquid this is not observed. This acts as a fingerprint of the ionic liquid constituent that, besides contributing with ionic species, provides greater internal mobility to the material, enhancing the response to the outer electrical field. To take advantage of the hybrid gels electrical conductivity properties, a second prototype e-nose was designed and assembled. Here, the hybrid gel films acted, simultaneously, as active layers in optical and electrical gas sensors (Figure S9, Supporting Information). One hybrid gel sensing slide (composition: gelatin, [BMIM][FeCl<sub>4</sub>], 5CB, and water) was positioned in the e-nose sensor array and exposed to vapors from mixtures of ethanol in gasoline at different concentrations (v/v) during seven cycles (5 s exposition followed by 55 s recovery) (Figure 5). The gel's relative admittance increased linearly upon exposure to the headspace of fuel mixtures with increasing ethanol content. When VOCs are adsorbed into the gel, the mobility of ions increases and therefore, the material's admittance increases. The increase of the ionic mobility might be related with an increase in fluidity due to a decrease of viscosity of the ionic liquid when it adsorbs organic molecules,<sup>[46]</sup> or with conformational changes in the polymer chains.<sup>[21]</sup> On the other hand, a linear decrease in the LDR relative conductance was observed after exposure to VOCs with increasing ethanol content (20%–80%) (Figure S10, Supporting Information). The lack of linearity for the higher concentration of ethanol in solution (80%–100%) can be explained by the effect of protic solvents on hybrid gels. Still, the electrical and optical signals could be simultaneously correlated with the concentration of ethanol in the fuel mixtures (20%–100%) by adjusting a multiple linear regression model ( $p < 0.005$ ; Figure 5B and Tables S2 and S3, Supporting Information). This shows that the combination of independently obtained electrical and optical data yields a better estimation of the ethanol concentration in gasoline samples, than when the electrical or optical signals are employed in an isolated manner. The quantification of ethanol in automotive fuel, in the concentration range tested, is of great need for auditing fuel adulteration, and to estimate the percentage of ethanol inside fuel tanks of flexible-fuel cars, as opposed to currently employed lambda sensors, which measure exhaust gases.

### 3. Conclusion

In summary, we introduce a class of cooperative hybrid gels incorporating stable droplets of LCs self-assembled in the presence of room temperature ionic liquids with surfactant-like

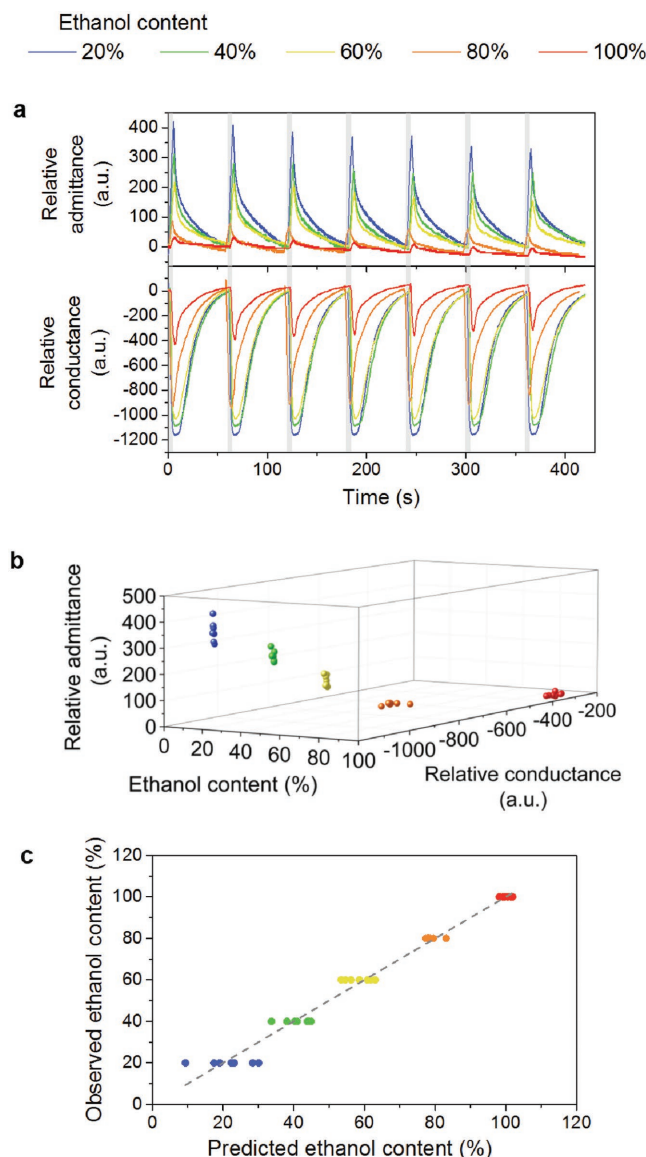


**Figure 5.** Application of a hybrid gel film as the active layer in optical and electrical gas sensors. a) Optical and electrical responses of the electronic nose using a single sensor with a hybrid gel, composed of gelatin, [BMIM]-[FeCl<sub>4</sub>], 5CB, and water, subjected to seven sequential exposure to vapors from different mixtures of ethanol in gasoline/air. Exposure periods highlighted in gray. b) 3D representation of the optical and electrical responses as a function of ethanol content in the fuel mixtures. c) Linear relation between the real (observed) ethanol content in the analyzed fuel mixtures and the ethanol content predicted using the equation determined in (b).

properties and biopolymers. The self-assembly properties result from the delicate control of noncovalent intermolecular interactions and create structures within structures, where each component has a cooperative effect in structure and function. The enormous versatility in the composition offers tailored physicochemical, morphological, mechanical, optical, and electrical properties. Hybrid gels can respond to chemical, physical, and mechanical stimuli, yielding both optical and electrical signals. Furthermore, they can be modified with targeting or functional species and easily molded in different formats and geometries.<sup>[47]</sup>



We provide proof-of-concept data to show that hybrid gels fulfill the potential of LCs in gas sensing due to the combinatorial nature and robustness of the materials. In addition, the LC-based gas sensing system here presented overcomes some drawbacks associated with the use of metal oxide semiconductors, namely high operating temperatures, use of toxic and often noxious reagents during fabrication, and limited stability.<sup>[48–50]</sup> The stimuli-responsive properties of hybrid gels can also be explored for chemical sensing in aqueous phases, for temperature and pressure sensitive materials, applied in vitro or in vivo.<sup>[51]</sup> Hybrid gels represent platform optoelectronic materials compatible with miniaturized, wireless and wearable devices, and with potential in a wide range of applications from plastic electronics to electrochemical and polymer-dispersed liquid-crystal (PDLC) devices.

## Supporting Information

Supporting Information is available from the Wiley Online Library or from the author.

## Acknowledgements

A.H. and A.T.S.S. contributed equally to this work. This work was supported by the European Research Council through the grant reference SCENT-ERC-2014-STG-639123 (2015–2020) and by the Unidade de Ciências Biomoleculares Aplicadas (UCIBIO), which is financed by national funds from Fundação para a Ciência e Tecnologia/Ministério da Educação e Ciência (FCT/ME) (UID/Multi/04378/2013) and cofinanced by the European Regional Development Fund under the PT2020 Partnership Agreement (POCI-01-0145-FEDER-007728). The authors thank Fundação para a Ciência e a Tecnologia, Portugal, for the research fellowships SFRH/BPD/34768/2007 for A.H. and SFRH/BPD/97585/2013 for A.S.P. and financed project RECI/BBB-BEP/0124/2012. The authors also acknowledge funding from Conselho Nacional de Desenvolvimento Científico e Tecnológico, Brazil (CNPq) through Processes 400740/2014-1 and 307915/2013-1, both for J.G., and 508207/2010-0 for B.F.M. The Faculdade de Ciências e Tecnologia, Universidade Nova de Lisboa (FCT-UNL) and Universidade de São Paulo (USP) have filed a patent application on technology related to the processes described in this article. Several authors are listed as inventors on the patent application. The authors are grateful to Prof. João Sotomayor from FCT-UNL, Portugal, for polarizing optical microscope images, to Dr. Gustavo P. Rehder from Escola Politécnica - USP, Brazil, for the interdigitated electrodes, to Prof. Omar A. El Seoud from Instituto de Química - USP for the ionic liquid sample ([ALOCIM][Cl]), to Renan I. Ishara from Escola Politécnica - USP, Brazil, for drawing Figure 4A,B, and to Prof. Maria João Romão from UCIBIO, FCT-UNL for access to the X-ray Diffraction facilities.

## Conflict of Interest

The authors declare no conflict of interest.

## Keywords

gas sensing, gelatin, ionic liquids, liquid crystals, self-assembly

Received: February 13, 2017

Revised: March 16, 2017

Published online: May 29, 2017

- [1] Q. Wang, J. L. Mynar, M. Yoshida, E. Lee, M. Lee, K. Okuro, K. Kinbara, T. Aida, *Nature* **2010**, 463, 339.
- [2] M. J. Webber, E. A. Appel, E. W. Meijer, R. Langer, *Nat. Mater.* **2016**, 15, 13.
- [3] Y. Y. Broza, P. Mochalski, V. Ruzsanyi, A. Amann, H. Haick, *Angew. Chem. Int. Ed.* **2015**, 54, 11036.
- [4] G. Peng, U. Tisch, O. Adams, M. Hakim, N. Shehada, Y. Y. Broza, S. Billan, R. Abdah-bortnyak, A. Kuten, H. Haick, *Nat. Nanotechnol.* **2009**, 4, 669.
- [5] A. R. V. Benvenho, R. W. C. Li, J. Gruber, *Sens. Actuators, B* **2009**, 136, 173.
- [6] K. Brudzewski, S. Osowski, W. Pawlowski, *Sens. Actuators, B* **2012**, 161, 528.
- [7] L. D. Bonifacio, G. A. Ozin, A. C. Arsenault, *Small* **2011**, 7, 3153.
- [8] D.-K. Lee, T. Yi, K.-E. Park, H.-J. Lee, Y.-K. Cho, S. J. Lee, J. Lee, J. H. Park, M.-Y. Lee, S. U. Song, S. W. Kwon, *Sci. Rep.* **2014**, 4, 6550.
- [9] S. Cong, T. Sugahara, T. Wei, J. Jiu, Y. Hirose, S. Nagao, K. Suganuma, *Adv. Mater. Interfaces*, **2016**, 3, 1600252.
- [10] S. Cong, T. Sugahara, T. Wei, J. Jiu, Y. Hirose, S. Nagao, K. Suganuma, *Cryst. Growth Des.* **2015**, 15, 4536.
- [11] R. Beccherelli, E. Zampetti, S. Pantalei, M. Bernabei, K. C. Persaud, *Sens. Actuators, B* **2010**, 146, 446.
- [12] B. R. Goldsmith, J. J. Mitala, J. Josue, A. Castro, M. B. Lerner, T. H. Bayburt, S. M. Khamis, R. A. Jones, J. G. Brand, S. G. Sligar, C. W. Luetje, A. Gelperin, P. A. Rhodes, B. M. Discher, A. T. C. Johnson, *ACS Nano* **2011**, 5, 5408.
- [13] M. Strauch, A. Lüdke, D. Münch, T. Laudes, C. G. Galizia, E. Martinelli, L. Lavra, R. Paolesse, A. Ulivieri, A. Catini, R. Capuano, C. Di Natale, *Sci. Rep.* **2014**, 4, 3576.
- [14] S. Ju, K.-Y. Lee, S.-J. Min, Y. K. Yoo, K. S. Hwang, S. K. Kim, H. Yi, *Sci. Rep.* **2015**, 5, 9196.
- [15] R. A. Potyrailo, R. K. Bonam, J. G. Hartley, T. A. Starkey, P. Vukusic, M. Vasudev, T. Bunning, R. R. Naik, Z. Tang, M. A. Palacios, M. Larsen, L. A. Le Tarte, J. C. Grande, S. Zhong, T. Deng, *Nat. Commun.* **2015**, 6, 1.
- [16] T. L. Greaves, C. J. Drummond, *Chem. Soc. Rev.* **2008**, 37, 1709.
- [17] R. Hayes, G. G. Warr, R. Atkin, *Chem. Rev.* **2015**, 115, 6357.
- [18] X. Wang, D. S. Miller, E. Bokusoglu, J. J. De Pablo, N. L. Abbott, *Nat. Mater.* **2015**, 15, 106.
- [19] A. Rehman, X. Zeng, *RSC Adv.* **2015**, 5, 58371.
- [20] P. V. Shibaev, M. Wenzlick, J. Murray, A. Tantillo, M. Wenzlick, J. Murray, A. Tantillo, *Mol. Cryst. Liq. Cryst.* **2016**, 611, 94.
- [21] T. Carvalho, P. Vidinha, B. R. Vieira, R. W. C. Li, J. Gruber, *J. Mater. Chem. C* **2014**, 2, 696.
- [22] V. K. Gupta, J. J. Skaife, T. B. Dubrovsky, N. L. Abbott, *Science* **1998**, 279, 2077.
- [23] A. Hussain, A. S. Pina, A. C. A. Roque, *Biosens. Bioelectron.* **2009**, 25, 1.
- [24] J. L. Adgate, A. Barteková, P. C. Raynor, J. G. Griggs, A. D. Ryan, B. R. Acharya, C. J. Volkmann, D. D. Most, S. Lai, M. D. Bonds, *J. Environ. Monit.* **2009**, 11, 49.
- [25] A. Sen, K. A. Kupcho, B. A. Grinwald, H. J. Vantreeck, B. R. Acharya, *Sens. Actuators, B* **2013**, 178, 222.
- [26] M. Bedolla-pantoja, N. L. Abbott, *ACS Appl. Mater. Interfaces* **2016**, 8, 13114.
- [27] X. Ding, K.-L. Yang, *Sens. Actuators, B* **2012**, 173, 607.
- [28] T. Kato, *Science* **2002**, 295, 2414.
- [29] R. J. Carlton, J. T. Hunter, D. S. Miller, R. Abbasi, P. C. Mushenheim, L. N. Tan, N. L. Abbott, *Liq. Cryst. Rev.* **2013**, 1, 29.
- [30] T. Bera, J. Deng, J. Fang, *RSC Adv.* **2015**, 5, 70094.
- [31] T. Bera, J. Fang, *Langmuir* **2013**, 29, 387.
- [32] K. Lee, C. Gupta, S. Park, I. Kang, *J. Mater. Chem. B* **2016**, 4, 704.
- [33] S. Sivakumar, K. L. Wark, J. K. Gupta, N. L. Abbott, F. Caruso, *Adv. Funct. Mater.* **2009**, 19, 2260.



- [34] D. S. Miller, X. Wang, J. Buchen, O. D. Lavrentovich, N. L. Abbott, *Anal. Chem.* **2013**, *85*, 10296.
- [35] Q. Hu, C. Jang, *Soft Matter* **2013**, *9*, 5779.
- [36] C. G. Reyes, A. Sharma, J. P. F. Lagerwall, *Liq. Cryst.* **2016**, *43*, 1986.
- [37] E. B. Kim, N. Lockwood, M. Chopra, O. Guzman, J. J. De Pablo, N. L. Abbott, *Biophys. J.* **2005**, *89*, 3141.
- [38] D. S. Miller, X. Wang, N. L. Abbott, *Chem. Mater.* **2014**, *26*, 496.
- [39] J. Deng, W. Liang, J. Fang, *ACS Appl. Mater. Interfaces* **2016**, *8*, 3928.
- [40] J. A. Moreno-Razo, E. J. Sambriski, N. L. Abbott, J. P. Hernández-Ortiz, J. J. de Pablo, *Nature* **2012**, *485*, 86.
- [41] P. Vidinha, N. M. T. Lourenço, C. Pinheiro, A. R. Brás, T. Carvalho, T. Santos-Silva, A. Mukhopadhyay, M. J. Romão, J. Parola, M. Dionísio, J. M. S. Cabral, C. A. M. Afonso, S. Barreiros, *Chem. Commun.* **2008**, *44*, 5842.
- [42] K. Rawat, J. Pathak, H. B. Bohidar, *Soft Matter* **2014**, *10*, 862.
- [43] J. Le Bideau, L. Viau, A. Vioux, *Chem. Soc. Rev.* **2011**, *40*, 907.
- [44] L. Gasperini, J. Mano, R. L. Reis, *J. R. Soc. Interface* **2014**, *11*, 20140817.
- [45] T. Carvalho, V. Augusto, A. R. Brás, N. M. T. Lourenço, C. A. M. Afonso, S. Barreiros, N. T. Correia, P. Vidinha, E. J. Cabrita, C. J. Dias, M. Dionísio, B. Roling, *J. Phys. Chem. B* **2012**, *116*, 2664.
- [46] X. Zhu, H. Zhang, J. Wu, *Sens. Actuators, B* **2014**, *202*, 105.
- [47] D. S. Miller, X. Wang, N. L. Abbott, *Chem. Mater.* **2014**, *26*, 496.
- [48] Z. Xie, K. Cao, Y. Zhao, L. Bai, H. Gu, H. Xu, Z.-Z. Gu, *Adv. Mater.* **2014**, *26*, 2413.
- [49] H. Lin, M. Jang, K. S. Suslick, *J. Am. Chem. Soc.* **2011**, *133*, 16786.
- [50] S. Chen, Y. Wang, S. Choi, *Open J. Appl. Biosens.* **2013**, *2*, 39.
- [51] A. Agarwal, E. Huang, S. Palecek, N. L. Abbott, *Adv. Mater.* **2008**, *20*, 4804.